Determination of the Electromagnetic Torque and Angular Velocity of an Induction Motor Based on Space Vectors

Tsvetozar Petkov
Department of Electric Power Distribution and Electrical Equipment
Technical University of Gabrovo
Gabrovo, Bulgaria
ORCID: 0009-0003-4368-7383

***Abstract*—This paper presents an analytical approach for determining the electromagnetic torque and angular velocity of a three-phase induction motor. The method is based on the space vectors of the motor's voltages and currents and requires the measurement of the instantaneous values of the stator voltages and currents. A study was conducted using a simulation developed in MATLAB/Simulink. The results obtained from the proposed method are compared with those from the asynchronous machine simulation model provided by the software package, demonstrating the accuracy and applicability of the approach.**

Keywords—angular velocity, electromagnetic torque, induction motor, space vector.

I. Introduction

A major focus in modern electric drive technology is the development of solutions that control electric motors with high energy efficiency and optimal mechanical characteristics [1]-[4]. In the control of induction motors, knowledge of the instantaneous values of the developed electromagnetic torque and rotor angular velocity is often required. These quantities can be obtained through direct measurement, which requires additional technical equipment, or by using mathematical methods that allow their computation in real time [5]-[18]. The aim of this paper is to present an analytical approach for determining the electromagnetic torque and angular velocity of an induction motor using space vector theory. Space vectors provide a fundamental framework for analyzing the transient and steady-state behavior of electric machines. Space vectors establish the relationship between the instantaneous values of the time-varying quantities and their spatial variation characteristics during the energy conversion process. In induction machines, the space vector approach provides a clear geometric visualization of the rotating magnetic field and allows straightforward calculation of the electromagnetic torque through a vector cross-product [19]-[24]. The proposed method presented in this paper was evaluated using the MATLAB/Simulink software environment [25], [26].

II. Determination of the Space Vectors and the Electromagnetic Torque

For induction machines, the main space vectors required are the stator phase voltage vector and the stator and rotor phase current vectors. Under conditions of electromagnetic symmetry, a single differential equation can be written for the electrical equilibrium in the stator circuits. This equation is formulated with respect to the three main space vectors, which rotate relative to the stationary stator at synchronous electrical speed $\omega_{0e} = 2\pi f$:

$$\overline{u}_S e^{j\omega_{0e}t} = \overline{i}_S e^{j\omega_{0e}t} R_S + L_S \frac{d\overline{i}_S e^{j\omega_{0e}t}}{dt} + L_m \frac{d\overline{i}_r e^{j\omega_{0e}t}}{dt}, \quad (1)$$

where: $\overline{u}_S = |\overline{u}_S| e^{j\varphi_{\overline{u}_S}}$ - stator voltage space vector; $\overline{i}_S = |\overline{i}_S| e^{j\varphi_{\overline{i}_S}}$ and $\overline{i}_r = |\overline{i}_r| e^{j\varphi_{\overline{i}_r}}$ - stator and rotor current space vectors; R_S - stator winding active resistance; L_S - stator total inductance; L_m - mutual inductance; $\varphi_{\overline{u}_S}$, $\varphi_{\overline{i}_S}$, $\varphi_{\overline{i}_r}$ - phase angles of the corresponding vectors.

In equation (1), the rotating space vectors $\overline{u}_S e^{j\omega_{0e}t}$ and $\overline{i}_S e^{j\omega_{0e}t}$ can be determined from the instantaneous measurements of the stator phase voltages and currents, as follows:

$$\overline{u}_S e^{j\omega_{0e}t} = k\left(u_A + u_B a + u_C a^2\right); \quad (2)$$

$$\overline{i}_S e^{j\omega_{0e}t} = k\left(i_A + i_B a + i_C a^2\right), \quad (3)$$

where: u_A, u_B, u_C and i_A, i_B, i_C - instantaneous values of the corresponding voltages and currents; $a = e^{j(2\pi/3)}$ - phase operator; $k = \sqrt{2/3}$ - proportionality coefficient.

The rotor current space vector is determined computationally. By differentiating $\overline{i}_S e^{j\omega_{0e}t}$ in equation (1), the derivative of the rotor current space vector can be expressed as:

$$\frac{d\overline{i}_r e^{j\omega_{0e}t}}{dt} = \frac{1}{L_m}\left(\overline{u}_S e^{j\omega_{0e}t} - \overline{i}_S e^{j\omega_{0e}t} R_S - L_S \frac{d\overline{i}_S e^{j\omega_{0e}t}}{dt}\right). \quad (4)$$

Equation (4) is subsequently integrated to obtain the rotor current vector $\overline{i}_r e^{j\omega_{0e}t}$. The resulting rotating vectors $\overline{i}_S e^{j\omega_{0e}t}$ and $\overline{i}_r e^{j\omega_{0e}t}$ are then multiplied by $e^{-j\omega_{0e}t}$, which allows for the determination of $\overline{i}_S$ and $\overline{i}_r$.

The electromagnetic torque can be expressed as a function of the stator and rotor current space vectors. Using the mutual inductance L_m, the torque is proportional to the imaginary

979-8-3315-5999-1/26/$31.00 ©2026 IEEE

part of the product between the stator current space vector and the complex conjugate of the rotor current space vector.

The electromagnetic torque T_e can be calculated using the following expression, based on the previously determined rotor and stator current space vectors:

$$T_e = pL_m \operatorname{Im}\left(\bar{i}_S \bar{i}_r^*\right), \tag{5}$$

where: p - number of pole pairs; $\bar{i}_r^*$ - complex conjugate of the rotor current space vector.

III. Determination of the Rotor Angular Velocity

The electrical balance in the rotor circuits, in the case of electromagnetic symmetry of the induction machine, can also be described by a single differential equation. This equation is formulated with respect to the previously determined space vectors of the stator and rotor currents, $\bar{i}_S$ and $\bar{i}_r$. These vectors rotate relative to the moving rotor at a speed $\omega_{0e} - \omega_e$, where ω_e is the rotor electrical speed:

$$0 = \bar{i}_r e^{j(\omega_{0e}-\omega_e)t} R_r' + L_m \frac{d\bar{i}_S e^{j(\omega_{0e}-\omega_e)t}}{dt} + L_r' \frac{d\bar{i}_r e^{j(\omega_{0e}-\omega_e)t}}{dt}, \tag{6}$$

where: R_r' - rotor winding resistance; L_r' - rotor total inductance.

By performing the necessary differentiations, equation (6) can be rationalized and expressed in the following form. This transformation provides a more convenient representation for computing the rotor angular velocity based on the previously determined stator and rotor current space vectors:

$$0 = \bar{i}_r R_r' + L_m \frac{d\bar{i}_S}{dt} + jL_m(\omega_{0e} - \omega_e)\bar{i}_S + L_r' \frac{d\bar{i}_r}{dt} + jL_r'(\omega_{0e} - \omega_e)\bar{i}_r. \tag{7}$$

Equation (7) is then expressed in an algebraic complex form, which facilitates the computation of the rotor angular velocity:

$$\begin{aligned} &R_r' \operatorname{Re}\left(\bar{i}_r\right) + L_m \operatorname{Re}\left(\frac{d\bar{i}_S}{dt}\right) - L_m(\omega_{0e} - \omega_e)\operatorname{Im}\left(\bar{i}_S\right) + \\ &+L_r' \operatorname{Re}\left(\frac{d\bar{i}_r}{dt}\right) - L_r'(\omega_{0e} - \omega_e)\operatorname{Im}\left(\bar{i}_r\right) + \\ &+j\left[\begin{array}{l} R_r' \operatorname{Im}\left(\bar{i}_r\right) + L_m \operatorname{Im}\left(\frac{d\bar{i}_S}{dt}\right) + L_m(\omega_{0e} - \omega_e)\operatorname{Re}\left(\bar{i}_S\right) + \\ +L_r' \operatorname{Im}\left(\frac{d\bar{i}_r}{dt}\right) + L_r'(\omega_{0e} - \omega_e)\operatorname{Re}\left(\bar{i}_r\right) \end{array}\right] = 0. \end{aligned} \tag{8}$$

By equating the real and imaginary parts, the equation is then solved with respect to the rotor electrical speed. The following expression is obtained:

$$\omega_e = \omega_{0e} - \frac{\begin{array}{l} R_r' \operatorname{Re}\left(\bar{i}_r\right) + L_m \operatorname{Re}\left(\frac{d\bar{i}_S}{dt}\right) + L_r' \operatorname{Re}\left(\frac{d\bar{i}_r}{dt}\right) - \\ L_m \operatorname{Re}\left(\bar{i}_S\right) + L_r' \operatorname{Re}\left(\bar{i}_r\right) + \end{array}}{\begin{array}{l} -R_r' \operatorname{Im}\left(\bar{i}_r\right) - L_m \operatorname{Im}\left(\frac{d\bar{i}_S}{dt}\right) - L_r' \operatorname{Im}\left(\frac{d\bar{i}_r}{dt}\right) \\ +L_m \operatorname{Im}\left(\bar{i}_S\right) + L_r' \operatorname{Im}\left(\bar{i}_r\right) \end{array}}. \tag{9}$$

Once the rotor electrical speed ω_e has been determined, the actual rotor mechanical speed ω_r can be calculated using the relationship between electrical and mechanical quantities. Specifically, the mechanical speed is obtained by dividing the electrical speed by the number of pole pairs of the machine, as follows:

$$\omega_r = \frac{\omega_e}{p}. \tag{10}$$

To assess the accuracy and validity of the proposed method, a simulation was developed using the MATLAB/Simulink software environment. The study is based on a simulation model of an asynchronous machine provided by the software package. This setup allows for a direct comparison between the results obtained from the proposed method and those generated by the standard simulation model. The general layout of the developed simulation is shown in Fig. 1.

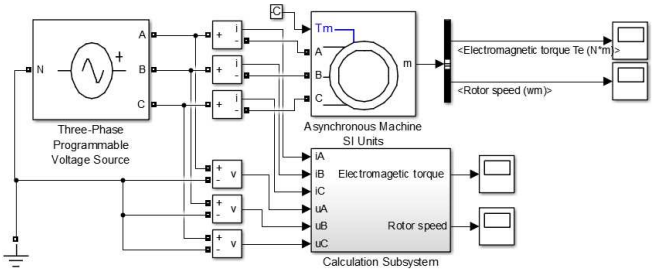


Fig. 1. General layout of the developed simulation.

The simulation model of the asynchronous machine has the following rated data: rated power $P_{rated} = 7.5\ kW$; rated line voltage $U_{rated} = 400\ V$; rated frequency $f_{rated} = 50\ Hz$; and rated rotational speed $N_{rated} = 1440\ \text{min}^{-1}$. The electromagnetic parameters of the machine are: $R_S = 0.7384\ \Omega$; $R_r' = 0.7402\ \Omega$; $L_S = L_r' = 0.127\ H$; and $L_m = 0.1241\ H$.

The results obtained using the proposed method are compared with those from the asynchronous machine simulation model to assess the accuracy and reliability of the approach. The study considers the case of a symmetrical stator voltage supply with rated RMS values and nominal load. Fig. 2 illustrates the variation of the developed electromagnetic torque obtained from the asynchronous machine simulation model, while Fig. 3 presents the corresponding results obtained using the proposed method. This comparison demonstrates the effectiveness of the proposed method in accurately reproducing the machine's dynamic behavior.

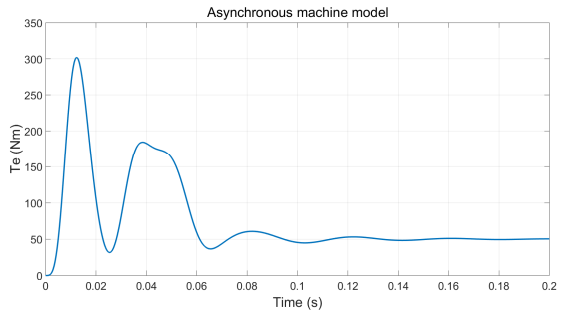


Fig. 2. Electromagnetic torque obtained from the asynchronous machine model.

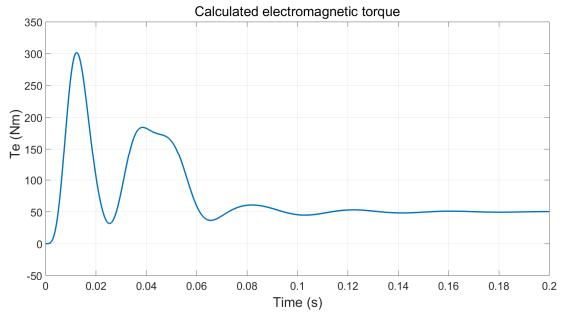


Fig. 3. Calculated electromagnetic torque.

The developed simulation illustrates the variation of the rotor angular velocity. Fig. 4 presents the results obtained from the asynchronous machine simulation model, while Fig. 5 shows the corresponding results obtained using the proposed method. This comparison highlights the ability of the proposed method to accurately reproduce the dynamic behavior of the rotor speed under nominal operating conditions.

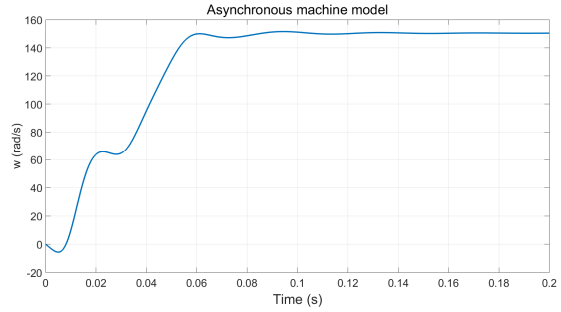


Fig. 4. Angular velocity obtained from the asynchronous machine model.

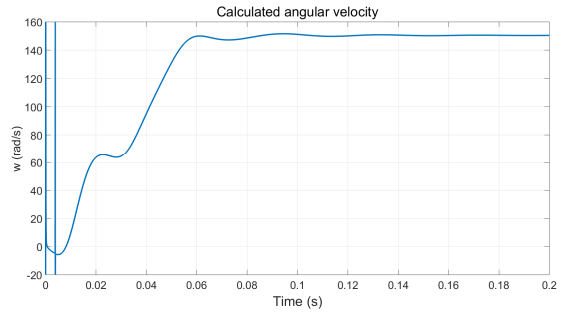


Fig. 5. Calculated angular velocity.

During the starting transient, the mathematical model contains singularities. The numerical simulation in MATLAB/Simulink, using an adaptive solver, successfully passes through these points by automatically reducing the integration step size and interpolating the solution, without evaluating the function exactly at the singular point.

In many cases, the induction motor operates under non-sinusoidal supply voltages. A typical example is when the motor is controlled by a semiconductor converter. In the motor control circuits, the semiconductor devices perform continuous switching operations, resulting in non-sinusoidal current waveforms.

The harmonic components of these non-sinusoidal currents generate equivalent rotating magnetic fields that rotate at different speeds and in different directions. These components produce counteracting torque components and adversely affect the overall performance of the machine. Under such conditions, the developed electromagnetic torque and the angular speed are not constant in steady state, and oscillations are observed. The fifth- and seventh-order harmonics are the most commonly encountered components. A characteristic feature of the fifth harmonic is that the equivalent electromagnetic field it produces rotates in the opposite direction to that of the fundamental harmonic field, whereas the field generated by the seventh harmonic rotates in the same direction as the fundamental field. To investigate the adequacy of the proposed method under non-sinusoidal conditions, fifth- and seventh-order harmonic components were introduced into the supply voltage waveforms. The amplitude of the fifth harmonic was set to 0.5 of the fundamental component, while the seventh harmonic was set to 0.3 of the fundamental. Fig. 6 presents the results obtained from the simulation model of the induction machine with respect to the developed electromagnetic torque, while Fig. 7 shows the results obtained using the proposed method. The motor was operating under rated load conditions.

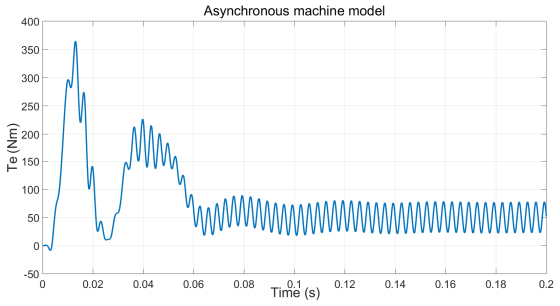


Fig. 6. Electromagnetic torque obtained from the asynchronous machine model.

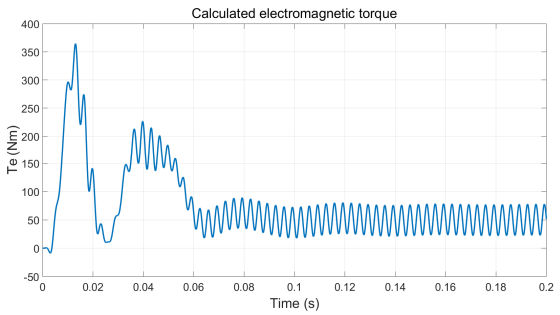


Fig. 7. Calculated electromagnetic torque.

The results obtained for the angular speed from the simulation model are shown in Fig. 8, while the results obtained using the proposed method are presented in Fig. 9.

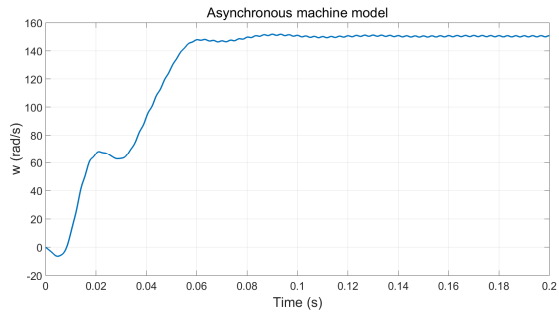


Fig. 8. Angular velocity obtained from the asynchronous machine model.

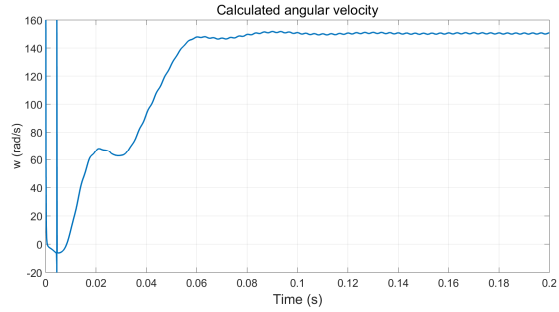


Fig. 9. Calculated angular velocity.

The study of the proposed method under different non-sinusoidal and unbalanced voltage conditions demonstrated results in agreement with the MATLAB/Simulink simulation model of the asynchronous machine.

IV. Conclusion

The results indicate that the proposed method can be effectively used to determine the electromagnetic torque and angular velocity of an induction motor during both transient and steady-state operating conditions. The method provides a reliable and computationally efficient approach for real-time monitoring and control of induction machines, making it suitable for practical applications in modern electric drive systems.

Acknowledgment

The author would like to express sincere gratitude to Technical University of Gabrovo for the excellent research environment, technical facilities, and institutional support provided during the development and preparation of this paper. This work was supported by a "Research, Analysis, and Optimization of the Energy Balance and Lighting Engineering Characteristics of Energy Facilities", № НИП2026-19.

References

[1] V. Klyuchev, Theory of Electric Drives, Tehnika, Sofia, 1989.

[2] J. A. Melkebeek, Electrical Machines and Drives. Fundamentals and Advanced Modelling, Springer Publishing, Germany, 2018.

[3] P. C. Krause, O. Wasynczuk and S. D. Sudhoff, Analysis of Electric Machinery and Drive Systems, IEEE Press Power Engineering Series, 2002.

[4] V. Hrabovcova, P. Rafajdus and P. Makys, Analysis of Electrical Machines, Intech Open, 2020.

[5] P. Liu, C.-Y. Hung, C.-S. Chiu, and K.-Y. Lian, ‘‘Sensorless linear induction motor control using fuzzy observers for speed tracking,’’ in Proc. IEEE Int. Conf. Robot. Autom., May 2010, pp. 5621–5626.

[6] Z. Yin, G. Li, Y. Zhang, and J. Liu, ‘‘Symmetric-strong-tracking-extended Kalman-filter-based sensorless control of induction motor drives for modeling error reduction,’’ IEEE Trans. Ind. Informat., vol. 15, no. 2, pp. 650–662, Feb. 2019.

[7] B. Chikondra, U. R. Muduli, and R. K. Behera, ‘‘An improved open-phase fault-tolerant DTC technique for five-phase induction motor drive based on virtual vectors assessment,’’ IEEE Trans. Ind. Electron., vol. 68, no. 6, pp. 4598–4609, Jun. 2021.

[8] J. K. Pandit, M. V. Aware, R. V. Nemade, and E. Levi, ‘‘Direct torque control scheme for a six-phase induction motor with reduced torque ripple,’’ IEEE Trans. Power Electron., vol. 32, no. 9, pp. 7118–7129, Sep. 2017.

[9] R. Bojoi, M. Lazzari, F. Profumo, and A. Tenconi, ‘‘Digital field-oriented control for dual three-phase induction motor drives,’’ IEEE Trans. Ind. Appl., vol. 39, no. 3, pp. 752–760, May 2003.

[10] V. S. Fating, S. V. Jadhav, R. T. Ugale, and B. N. Chaudhari, ‘‘Direct torque control of symmetrical and asymmetrical single phase induction motor,’’ in Proc. IEEE Power India Conf., Oct. 2008, pp. 1–4.

[11] M. Barut, R. Demir, E. Zerdali, and R. Inan, ‘‘Real-time implementation of bi input-extended Kalman filter-based estimator for speed-sensorless control of induction motors,’’ IEEE Trans. Ind. Electron., vol. 59, no. 11, pp. 4197–4206, Nov. 2012.

[12] E. R. Montero, M. Vogelsberger, and T. Wolbank, “Robust saliency based speed sensorless control of induction machines under overload operation,” in Proc. Int. Conf. Electr. Mach. (ICEM), Valencia, Spain, Sep. 2022, pp. 586–591, doi: 10.1109/ICEM51905.2022. 9910761.

[13] D. A. Dominic and T. R. Chelliah, ‘‘Analysis of field-oriented controlled induction motor drives under sensor faults and an overview of sensorless schemes,’’ ISA Trans., vol. 53, no. 5, pp. 1680–1694, Sep. 2014.

[14] I. M. Alsofyani and N. R. N. Idris, ‘‘A review on sensorless techniques for sustainable reliability and efficient variable frequency drives of induction motors,’’ Renew. Sustain. Energy Rev., vol. 24, pp. 111–121, Aug. 2013.

[15] M. H. Holakooie, M. Ojaghi, and A. Taheri, ‘‘Direct torque control of six-phase induction motor with a novel MRAS-based stator resistance estimator,’’ IEEE Trans. Ind. Electron., vol. 65, no. 10, pp. 7685–7696, Oct. 2018.

[16] S. Di Gennaro, J. R. Dominguez, and M. A. Meza, ‘‘Sensorless high order sliding mode control of induction motors with core loss,’’ IEEE Trans. Ind. Electron., vol. 61, no. 6, pp. 2678–2689, Jun. 2014.

[17] A. Khedher and M. Faouzi Mimouni, ‘‘Sensorless-adaptive DTC of double star induction motor,’’ Energy Convers. Manage., vol. 51, no. 12, pp. 2878–2892, Dec. 2010.

[18] Y. Yu, X. Huang, B. Wang, H. Bu, C. Chen, and D. Xu, ‘‘Speed-sensorless vector control with single phase current sensor for induction motor drives using current compensation method,’’ in Proc. 21st Int. Conf. Electr. Mach. Syst. (ICEMS), Jeju, South Korea, Oct. 2018, pp. 1590–1594.

[19] V. Dinov, Unsymmetrical Modes and Transients in Electrical Machines, Tehnika, Sofia, 1974.

[20] T. Petkov, “Simplified mathematical model of an induction motor,” IEEE, 23rd International Symposium on Electrical Apparatus and Technologies (SIELA), Bourgas, Bulgaria, 2024, pp: 1-4. ISBN 979-8-3503-8236-5.

[21] U. R. Muduli, B. Chikondra, and R. K. Behera, ‘‘Space vector PWM based DTC scheme with reduced common mode voltage for five-phase induction motor drive,’’ IEEE Trans. Power Electron., vol. 37, no. 1, pp. 114–124, Jan. 2022, doi: 10.1109/TPEL.2021.3092259.

[22] M. A. Jabbar, A. M. Khambadkone, and Z. Yanfeng, ‘‘Space-vector modulation in a two-phase induction motor drive for constant-power operation,’’ IEEE Trans. Ind. Electron., vol. 51, no. 5, pp. 1081–1088, Oct. 2004.

[23] Y. V. S. Reddy, T. B. Reddy, and M. V. Kumar, ‘‘A new space vector pulse width modulation for reduction of common mode voltage in direct torque controlled induction motor drive,’’ in Proc. Int. Conf. Power Electron., Drives Energy Syst., Dec. 2006, pp. 1–5.

[24] M. M. A. and B. Jacob, “A new space vector pulse density modulation scheme for two-level five phase induction motor drive,” IEEE Trans. Ind. Electron., vol. 69, no. 12, pp. 12077–12085, Dec. 2022.

[25] J. Tonchev, MATLAB 6-7 Conversion, Calculations, Visualization, Part II, Tehnika, Sofia, 2008.

[26] E. Hossain, MATLAB and Simulink Crash Course for Engineers. Springer International Publishing, Oregon Institute of Technology, 2022.